Supplementary Information

Atmospheric Fate of Methyl Isocyanate, CH_3NCO: OH and Cl Reaction Kinetics and Identification of Formyl Isocyanate, HC(O)NCO

Dimitrios K. Papanastasiou[1,2,&], François Bernard[1,2,#], and James B. Burkholder[1]

[1] Chemical Sciences Laboratory, National Oceanic and Atmospheric Administration, 325 Broadway, Boulder, CO, USA 80305-3328

[2] Cooperative Institute for Research in Environmental Sciences, University of Colorado, Boulder, CO, USA 80309

[&] Current address: Buffalo Research Laboratories, Honeywell International Inc., 20 Peabody St., Buffalo NY 14210 USA

Current address: Laboratoire de Physique et Chimie de l'Environnement et de l'Espace (LPC2E), Centre National de la Recherche Scientifique (CNRS), Université d'Orléans, Observatoire des Sciences de l'Univers en région Centre - Val de Loire (OSUC), Orléans, France

*Corresponding author: James B. Burkholder

e-mail: James.B.Burkholder@noaa.gov

Phone: (303)-497-3252

ORCID: 0000-0001-9532-6246

Infrared Absorption Spectrum

The infrared absorption spectrum of methyl isocyanate (CH_3NCO, MIC) at 295 K measured in this work is shown in **Figure S1**. The CH_3NCO spectra was acquired using independently prepared dilute mixtures of CH_3NCO in He (mixing ratio ranged from 0.316 to 3.48%), different absorption pathlengths (15, 125, 305, and 485 cm), as well as with measurements performed under static or flow conditions were in good agreement, to within ~4%. The infrared spectrum was independent of total pressure (He bath gas) over the 5 and 320 Torr range. The infrared spectrum of CH_3NCO shows a strong absorption band between 2200 and 2400 cm^{-1}, which is characteristic of the isocyanate functionality.[1]

The absorption band strength for the 1900–2700 cm^{-1} region is $(1.58 \pm 0.02) \times 10^{-16}$ cm^2 $molecule^{-1}$ cm^{-1}, where the uncertainty is the fit precision, as determined by a linear least-squares fit of the integrated absorbance versus [CH_3NCO] × Pathlength (see **Figure S2**). The CH_3NCO infrared spectrum from the infrared database of the Pacific Northwest Laboratory[2] is in good agreement (to within 5%) with the spectrum from this work. Note that the CH_3NCO gas mixtures used for the measurements contained <3% TMCS and <0.1% HMDS and the infrared spectrum reported here was corrected for those impurities using reference spectra. We should also note that the CH_3NCO absorption band in the 1900–2700 cm^{-1} region is free of any contribution from TMCS and HMDS.

UV Absorption Spectrum

The UV absorption spectrum of CH_3NCO, measured at 295 K in this work is shown in **Figure S3**. The spectrum at intervals of 0.5 nm is given in **Table S1**. At 200 nm the cross section is $(2.40 \pm 0.06) \times 10^{-19}$ cm^2 $molecule^{-1}$ and seems to be in the tail of a shorter wavelength excitation, while at ~215 nm a weaker transition is observed. At wavelengths greater than 230 nm, the spectrum decreases monotonically. The UV spectra measurements did not show any significant absorption (cross sections are below 1×10^{-21} cm^2 $molecule^{-1}$) for wavelengths longer than 260 nm. The precision of the data is better than 3% from 200 to 230 nm, while at longer wavelengths the uncertainty increases to ~10% at 250 nm.

UV spectra measurements were performed using a TMCS/He gas mixtures with known HMDS impurities (<3%). Using the latter gas mixture at similar concentrations to what is expected in the CH_3NCO/He gas mixtures it was shown that TMCS and HMDS make a negligible

contribution (<0.1%) to the observed CH_3NCO absorption for the wavelength range between 200 and 260 nm.

The Beer's law plot for CH_3NCO at 184.9 nm is shown in **Figure S4**. The absorption cross section of CH_3NCO at 184.9 nm is $(1.95 \pm 0.02) \times 10^{-18}$ cm^2 molecule^{-1} and was determined with measurements using 2 different gas mixtures of CH_3NCO in He as well as 2 different absorption path lengths (25 and 100 cm). On the basis of the complementary infrared measurements, the gas mixtures contained <3% TMCS and <0.1% HMDS, which would make a negligible contribution (<1%) to the absorption measurement based on available 184.9 nm absorption cross section data for TMCS (2.2×10^{-19} cm^2 molecule^{-1}) and HMDS (8.99×10^{-18} cm^2 molecule^{-1}).[3,4] The absorption cross section at 184.9 nm reported in this work is in good agreement with the value of 2×10^{-18} cm^2 molecule^{-1} reported in the study of Tokue et al., where the VUV absorption of CH_3NCO was measured.[5]

Table S1. UV absorption cross sections for methyl isocyanate (CH_3NCO) at 296 K obtained in this work between 200 and 260 nm. Uncertainties are the 2σ precision of the measurement.

λ (nm)	σ (10^{-20} cm^2 molecule^{-1})	Uncertainty (10^{-20} cm^2 molecule^{-1})	λ (nm)	σ (10^{-20} cm^2 molecule^{-1})	Uncertainty (10^{-20} cm^2 molecule^{-1})
200.0	24.0	0.6	230.5	2.63	0.04
200.5	22.4	0.5	231.0	2.53	0.03
201.0	21.1	0.4	231.5	2.43	0.04
201.5	19.7	0.4	232.0	2.34	0.03
202.0	18.5	0.3	232.5	2.25	0.03
202.5	17.3	0.3	233.0	2.16	0.03
203.0	16.3	0.3	233.5	2.07	0.03
203.5	15.4	0.2	234.0	1.99	0.03
204.0	14.5	0.2	234.5	1.91	0.03
204.5	13.7	0.2	235.0	1.83	0.03
205.0	13.0	0.2	235.5	1.75	0.03
205.5	12.3	0.2	236.0	1.68	0.03
206.0	11.7	0.2	236.5	1.61	0.03
206.5	11.2	0.2	237.0	1.53	0.03
207.0	10.7	0.2	237.5	1.47	0.03
207.5	10.3	0.2	238.0	1.40	0.02
208.0	9.85	0.15	238.5	1.34	0.03
208.5	9.48	0.14	239.0	1.28	0.03
209.0	9.14	0.14	239.5	1.22	0.03
209.5	8.83	0.13	240.0	1.17	0.03
210.0	8.54	0.13	240.5	1.11	0.03
210.5	8.28	0.12	241.0	1.06	0.03
211.0	8.03	0.12	241.5	1.01	0.03
211.5	7.80	0.12	242.0	0.962	0.028
212.0	7.59	0.12	242.5	0.916	0.033
212.5	7.39	0.11	243.0	0.873	0.031
213.0	7.20	0.11	243.5	0.831	0.034
213.5	7.02	0.10	244.0	0.790	0.033
214.0	6.84	0.10	244.5	0.751	0.032
214.5	6.68	0.09	245.0	0.716	0.034
215.0	6.52	0.09	245.5	0.677	0.032
215.5	6.37	0.09	246.0	0.645	0.035
216.0	6.22	0.09	246.5	0.611	0.034
216.5	6.06	0.09	247.0	0.581	0.034
217.0	5.93	0.08	247.5	0.550	0.032
217.5	5.79	0.08	248.0	0.522	0.036
218.0	5.65	0.08	248.5	0.495	0.034
218.5	5.51	0.08	249.0	0.470	0.035
219.0	5.37	0.08	249.5	0.446	0.037
219.5	5.24	0.07	250.0	0.422	0.036
220.0	5.11	0.07	250.5	0.399	0.037
220.5	4.98	0.06	251.0	0.381	0.036
221.0	4.85	0.06	251.5	0.358	0.035
221.5	4.72	0.07	252.0	0.337	0.037
222.0	4.59	0.06	252.5	0.321	0.038
222.5	4.46	0.06	253.0	0.304	0.036
223.0	4.34	0.06	253.5	0.289	0.038
223.5	4.21	0.05	254.0	0.271	0.037
224.0	4.09	0.05	254.5	0.257	0.037
224.5	3.96	0.06	255.0	0.242	0.036
225.0	3.84	0.05	255.5	0.228	0.037
225.5	3.72	0.05	256.0	0.217	0.039
226.0	3.60	0.05	256.5	0.204	0.037
226.5	3.49	0.05	257.0	0.191	0.035
227.0	3.37	0.04	257.5	0.181	0.035
227.5	3.26	0.05	258.0	0.173	0.034
228.0	3.15	0.04	258.5	0.162	0.036
228.5	3.04	0.04	259.0	0.155	0.040
229.0	2.93	0.04	259.5	0.144	0.034
229.5	2.83	0.04	260.0	0.134	0.036
230.0	2.73	0.04			

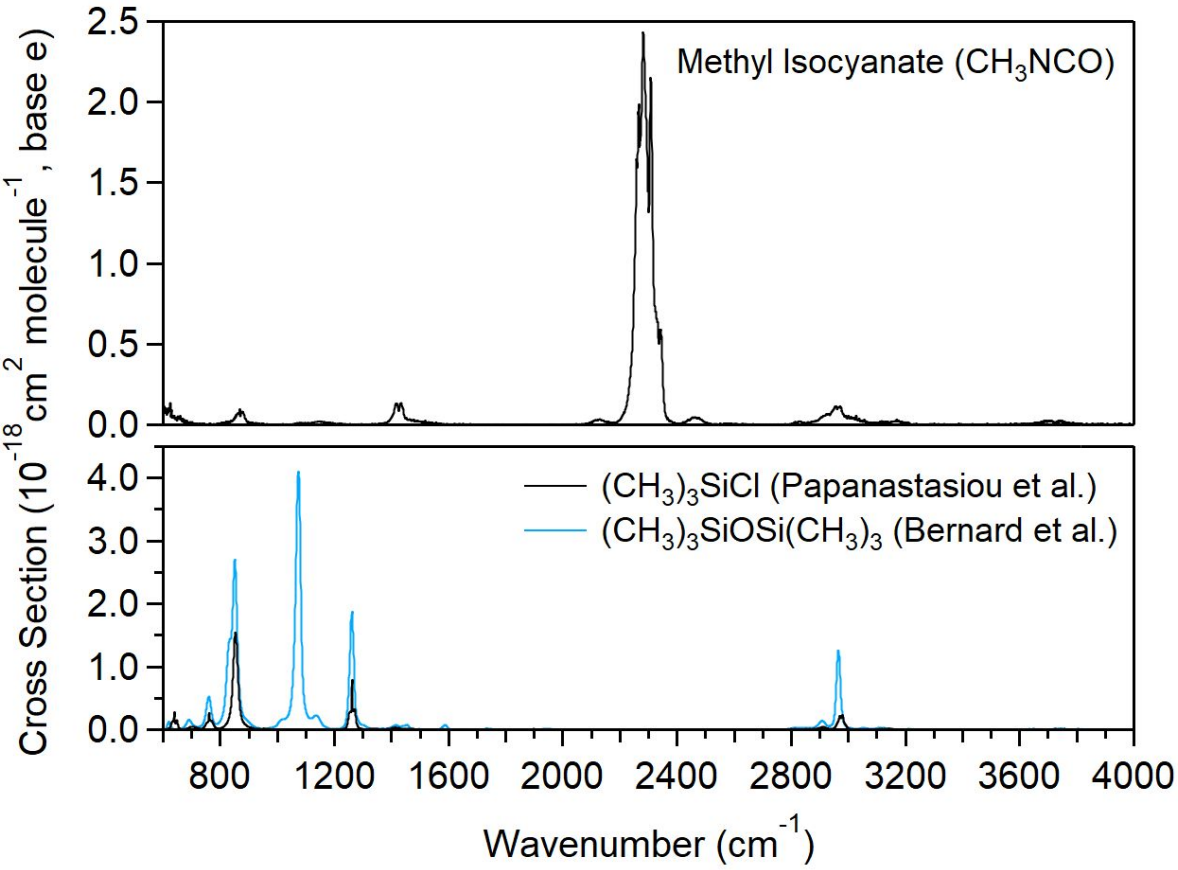

Figure S1. (a) Infrared absorption spectrum of methyl isocyanate, CH_3NCO, measured in this work at 1 cm^{-1} resolution. (b) Infrared absorption spectrum of trimethylchlorosilane, $(CH_3)_3SiCl$, taken from Papanastasiou et al.[6] at 1 cm^{-1} resolution and that of hexamethyldisiloxane, $(CH_3)_3SiOSi(CH_3)_3$, taken from Bernard et al.[7]

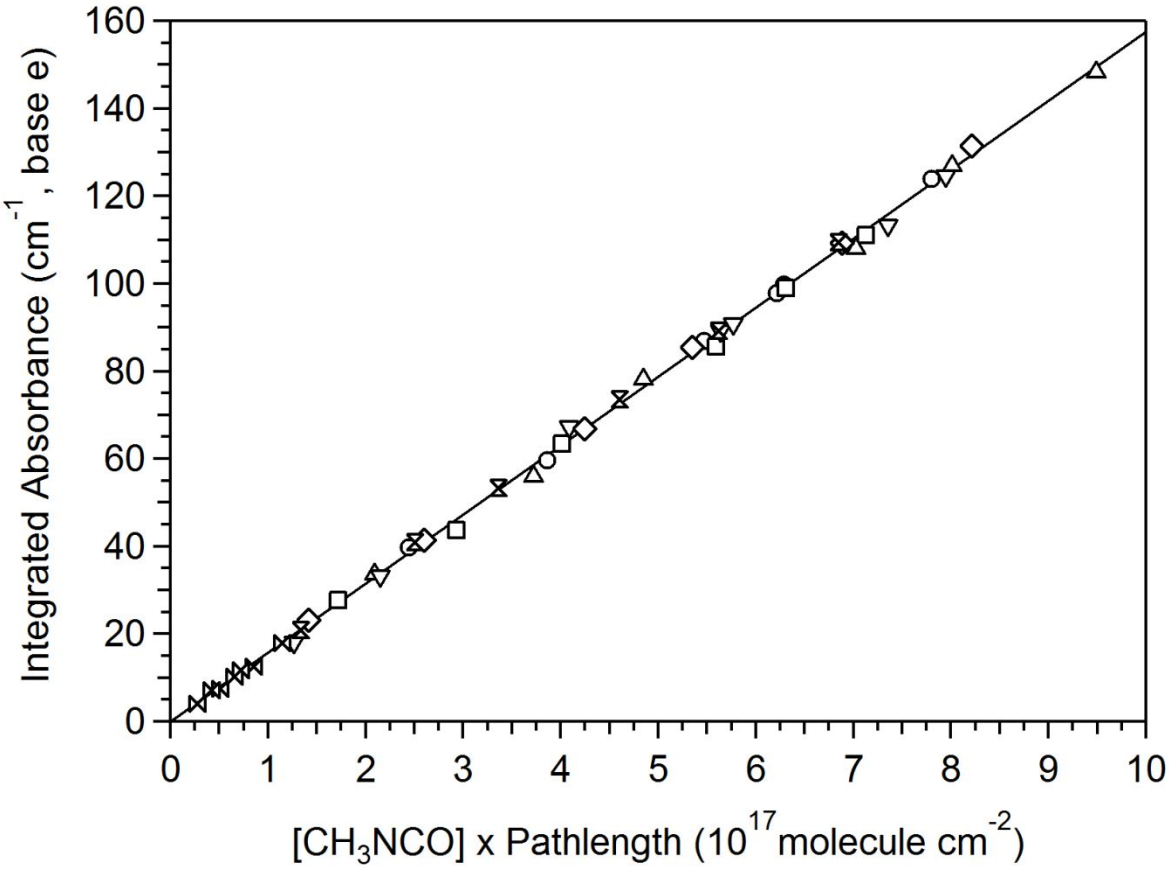

Figure S2. CH_3NCO absorption band strength between 1900 and 2700 cm^{-1} measured in this work. The different symbols represent measurements with different mixtures of CH_3NCO in He (mixing ratio ranged from ~0.3 to ~3%), different absorption cell pathlengths (15, 125, 305, and 485 cm), as well as with measurements done under static or flow conditions.

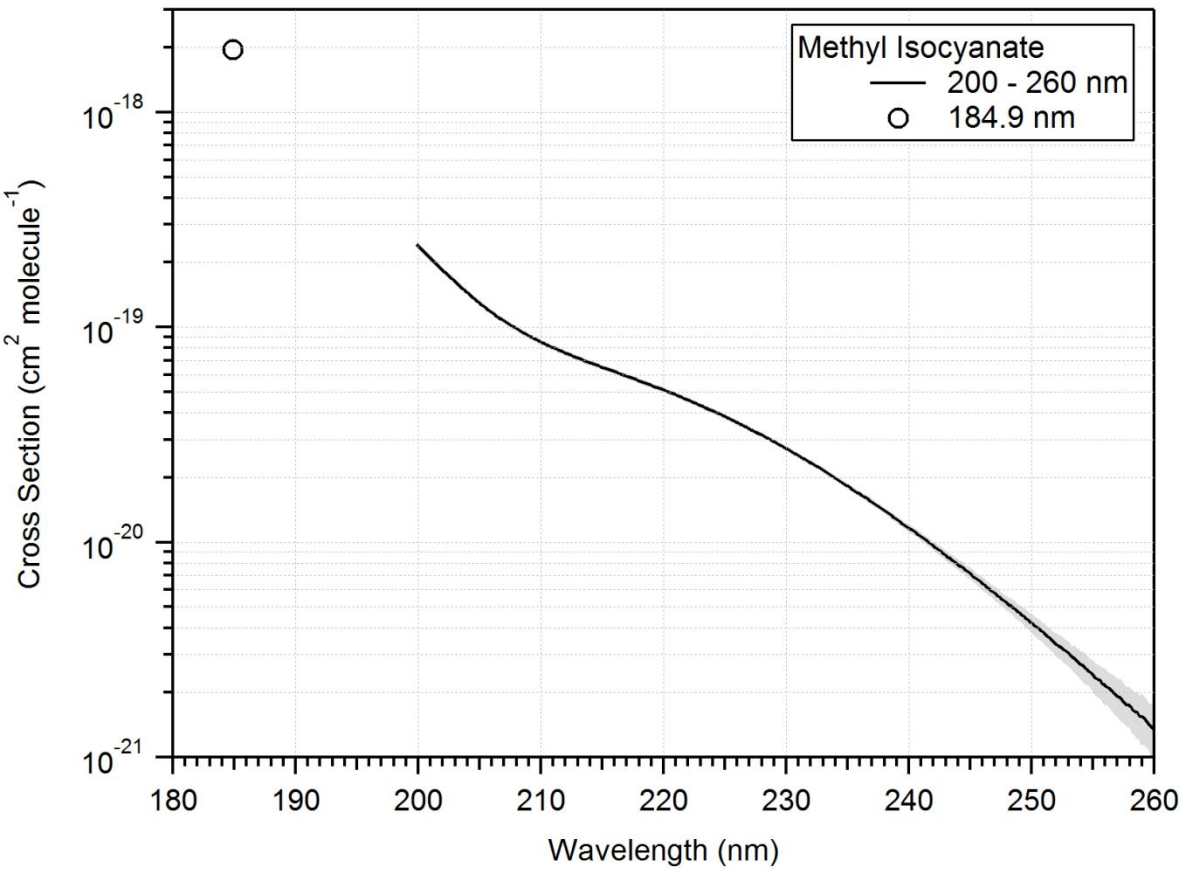

Figure S3. CH_3NCO UV absorption spectrum between 200 and 260 nm and at 184.9 nm measured in this work. The limits of the grey shaded region are the estimated 2σ precision of the measurement (see **Table S1**). The estimated 2σ precision for the 184.9 nm cross section measurements is ~1%.

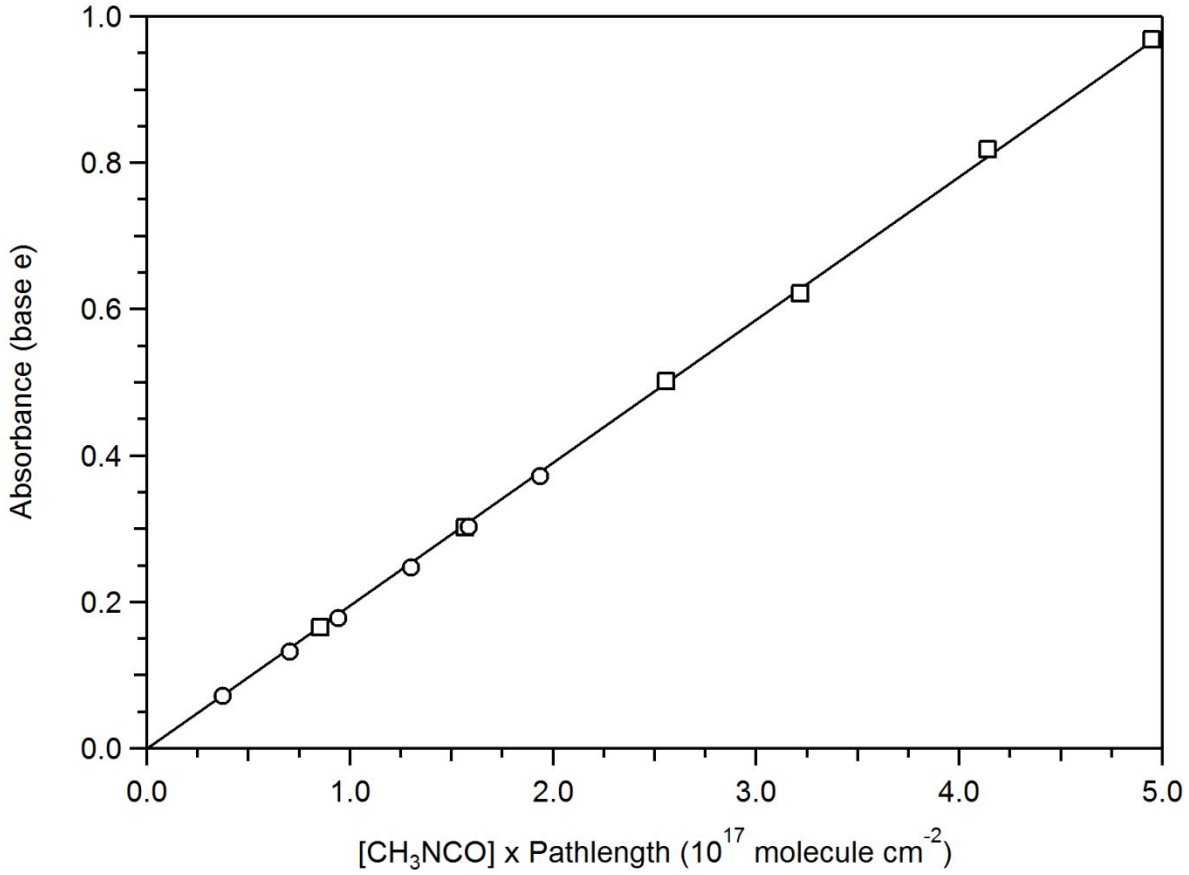

Figure S4. CH_3NCO 184.9 nm absorption cross section determination data. Measurements were made using two independently prepared dilute gas mixtures of CH_3NCO in He, 3.48% (circles) and 3.09 % (squares), and absorption cells with pathlengths of 25 and 100 cm, respectively.

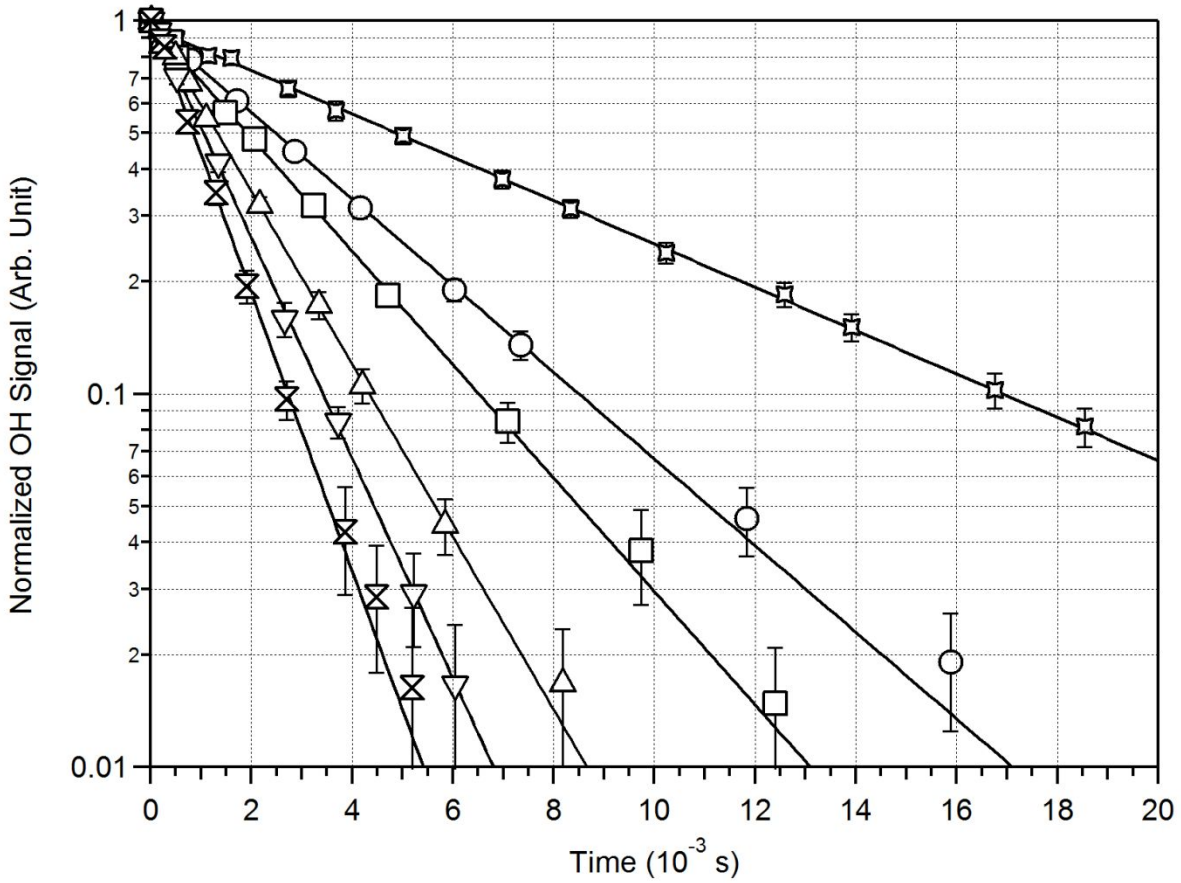

Figure S5. Representative normalized OH temporal profiles measured in this work for the OH + CH_3NCO reaction using the PLP–LIF technique at 296 K and 100 Torr total pressure (He bath gas). The OH decays were measured with [CH_3NCO] (10^{15} molecule cm^{-3}): 0, 0.87, 1.38, 2.56, 3.68, and 4.90 in the order of increasing slope. The lines are least-squares fit and the data error bars are the 1σ measurement precision.

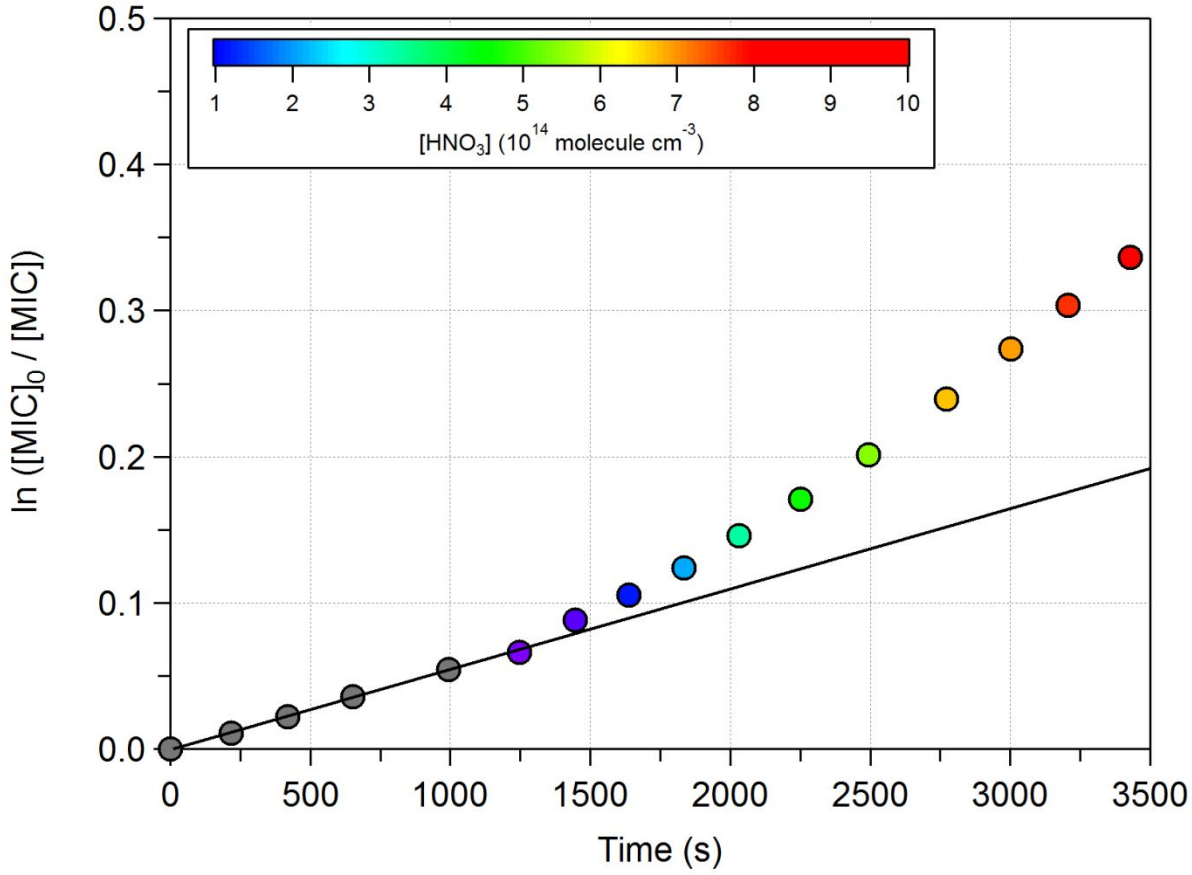

Figure S6. Loss of CH_3NCO, followed by infrared spectroscopy, with and without HNO_3 present in the reactor. The initial data (grey points) is the loss of CH_3NCO without HNO_3 present (the linear least-squares fit to the data is shown with the black line). The increased loss of CH_3NCO in the presence of HNO_3 is shown with the colored data points where the color scale represents $[HNO_3]$.

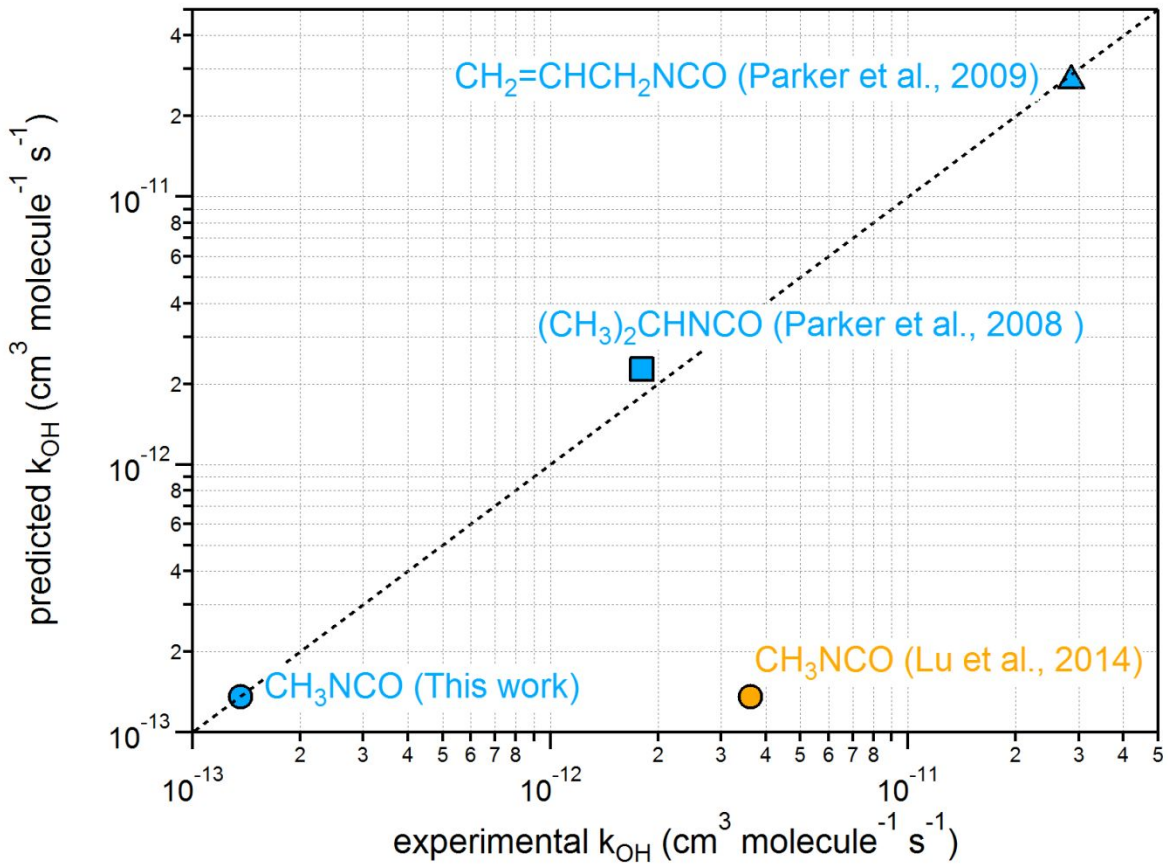

Figure S7. Comparison of the predicted OH rate coefficients, at 298 K, for methyl isocyanate, CH_3NCO, isopropyl isocyanate, $(CH_3)_2CHNCO$, and allyl isocyanate, (CH_2=$CHCH_2NCO$) using the structure activity relationship of Kwok and Atkinson[8] with the experimentally determined values from this and previous work.[9,10] The dashed line represents the 1:1 relationship. For comparison, the OH rate coefficient for CH_3NCO from the work of Lu et al. [11] is included.

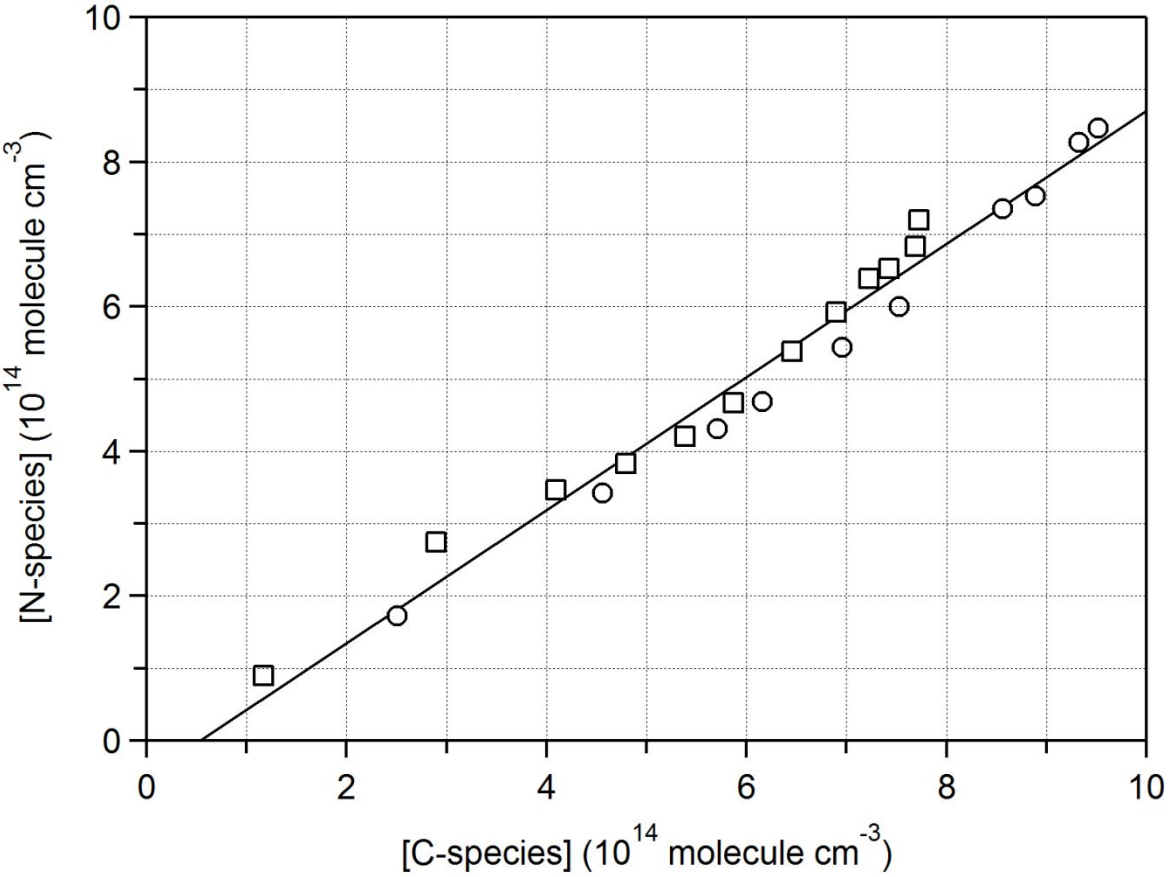

Figure S8. Sum of nitrogen species mass (calculated as 2 N_2O + HNCO + HC(O)NCO) compared with the sum of carbon species mass (calculated as ½ CO + ½ CO + ½ HNCO + HC(O)NCO). The data included in the analysis are from the OH (circles) and Cl (squares) initiated oxidation experiments. The solid line is a linear least-squares fit of the data with a slope of 0.92 ± 0.06.

References:

(1) Hirschmann, R. P.; Kniseley, R. N.; Fassel, V. A. The infrared spectra of alkyl isocyanates. *Spectrochimica Acta* **1965**, *21*, 2125-2133.

(2) Sharpe, S. W.; Johnson, T. J.; Sams, R. L.; Chu, P. M.; Rhoderick, G. C.; Johnson, P. A. Gas-phase databases for quantitative infrared spectroscopy. *App. Spectrosc.* **2004**, *58*, 1452-1461.

(3) Roberge, R.; Sandorfy, C.; Strausz, O. P. The electronic spectra of the alkyl, fluorine and chlorine substituted derivatives of silane. *Theoretica chimica acta* **1979**, *52*, 171-179.

(4) Bernard, F.; Papanastasiou, D. K.; Papadimitriou, V. C.; Burkholder, J. B. Temperature dependent rate coefficients for the gas-phase reaction of the OH radical with linear (L2, L3) and cyclic (D3, D4) permethylsiloxanes. *J. Phys. Chem. A* **2018**, *122*, 4252-4264.

(5) Tokue, I.; Hiraya, A.; Shobatake, K. Photoexcitation of CH_3NCO, CH_3NCS and CH_3SCN in the vacuum ultraviolet: Rydberg states and photofragment emission. *CHem. Phys.* **1987**, *117*, 315-324.

(6) Papanastasiou, D. K.; Bernard, F.; Burkholder, J. B. Trimethylchlorosilane, $(CH_3)_3SiCl$: OH reaction kinetics and infrared spectrum. *Int. J. Chem. Kinet.* **2020**, 1-6.

(7) Bernard, F.; Papanastasiou, D. K.; Papadimitriou, V. C.; Burkholder, J. B. Infrared absorption spectra of linear (L2 –L5) and cyclic (D3–D6) permethylsiloxanes. *J. Quant. Spec. Rad. Trans.* **2017**, *202*, 247-254.

(8) Kwok, E. S. C.; Atkinson, R. Estimation of hydroxyl radical reaction rate constants for gas-phase organic compounds using a structure-reactivity relationship: An update. *Atmos. Environ.* **1995**, *29*, 1685-1695.

(9) Parker, J. K.; Espada-Jallad, C. Kinetics of the gas-phase reactions of OH and NO_3 radicals and O_3 with allyl alcohol and allyl isocyanate. *J. Phys. Chem. A* **2009**, *113*, 9814-9824.

(10) Parker, J. K.; Espada-Jallad, C.; Parker, C. L.; Witt, J. D. Measurement and calculation of the rate constant for the reaction of isopropyl isocyanate with hydroxyl radical. *Int. J. Chem. Kinet.* **2009**, *41*, 187-197.

(11) Lu, Z.; Hebert, V. R.; Miller, G. C. Gas-phase reaction of methyl isothiocyanate and methyl isocyanate with hydroxyl radicals under static relative rate conditions. *J. Agricul. Food Chem.* **2014**, *62*, 1792-1795.